

1 The role of the CipA scaffoldin protein in  
2 cellulose solubilization as determined by  
3 targeted gene deletion and  
4 complementation in *Clostridium*  
5 *thermocellum*

---

6 Running title: CipA deletion and complementation in *C. thermocellum*

7 Daniel G. Olson<sup>1,4</sup>, Richard J. Giannone<sup>2,4</sup>, Robert L. Hettich<sup>2,4</sup> and Lee R. Lynd<sup>1,2,3,4</sup>#

8 <sup>1</sup>Dartmouth College, Hanover, NH 03755

9 <sup>2</sup>Oak Ridge National Laboratory, Oak Ridge, TN 37830

10 <sup>3</sup>Mascoma Corporation, Lebanon, NH 03766

11 <sup>4</sup>BioEnergy Science Center, Oak Ridge, TN 37830

12 # to whom correspondence should be addressed

13 lee.lynd@dartmouth.edu

## 14 **Abstract**

15 The CipA scaffoldin protein plays a key role in the *C. thermocellum* cellulosome. Previous  
16 studies have revealed that mutants deficient in binding or solubilizing cellulose also exhibit  
17 reduced expression of CipA. To confirm that CipA is, in fact, necessary for rapid solubilization of  
18 crystalline cellulose, the gene was deleted from the chromosome using targeted gene deletion  
19 technologies. The CipA deletion mutant exhibited a 100-fold reduction in cellulose  
20 solubilization rate, although it was eventually able to solubilize 80% of the 5 g/l cellulose  
21 initially present. The deletion mutant was complemented by a copy of *cipA* expressed from a  
22 replicating plasmid. In this strain, Avicelase activity was restored, although the rate was 2-fold  
23 slower than that of the wild type and the duration of the lag phase was increased. The *cipA*  
24 coding sequence is located at the beginning of a gene cluster containing several other genes  
25 thought to be responsible for the structural organization of the cellulosome, including *olpB*,  
26 *orf2p* and *olpA*. Tandem mass spectrometry revealed a 10-fold reduction in the expression of  
27 *olpB*, which may explain the slower growth rate. This deletion experiment adds further  
28 evidence that CipA plays a key role in cellulose solubilization by *C. thermocellum*, and raises  
29 interesting questions about the differential roles of the anchor scaffoldin proteins OlpB, Orf2p  
30 and SdbA.

## 31 **Introduction**

32 *Clostridium thermocellum* is an anaerobic thermophilic bacterium noted for its ability to rapidly  
33 solubilize crystalline cellulose, a process mediated by the cellulosome (1). The cellulosome is  
34 composed of tightly-bound enzymatic and structural components. At the heart of the

35 cellulosome is the scaffoldin protein, CipA (also known as S<sub>L</sub> and S1) (2). This protein has been  
36 shown to be capable of crystalline cellulose solubilization in conjunction with cellulosomal  
37 cellulase Cel48S (3). Analysis of the DNA sequence of *cipA* has revealed a set of nine repeated  
38 elements known as type I cohesins (4). These cohesins, bind to the type I dockerins found on  
39 cellulosomal enzymes (5). Subsequent analysis of the CipA protein has revealed three  
40 additional modules, the type II dockerin, the cellulose binding module (CBM) and the x-domain.  
41 The type II dockerin comprises a duplicated set of 22 amino acid residues located near the C-  
42 terminus of CipA (4). The type II dockerin binds to type II cohesins located on the anchor  
43 scaffoldin proteins, OlpB, Orf2p and SdbA. OlpB has seven type II cohesins, while Orf2p has two  
44 and SdbA has one. The anchor scaffoldins have a C-terminal sequence called the SLH domain  
45 that mediates binding to the cell surface(6). In CipA the CBM is located between the 2<sup>nd</sup> and 3<sup>rd</sup>  
46 type I cohesins and binds to crystalline cellulose with a K<sub>D</sub> of 0.4 μM (1). Thus the current  
47 understanding of the adhesion of *C. thermocellum* to cellulose involves the following 3  
48 interactions:

- 49 1. Binding of glycoside hydrolase enzymes in proximity to each other to promote enzyme-  
50 enzyme synergy.
- 51 2. Binding of enzymes to the cellulosic substrate via the CBM.
- 52 3. Anchoring the cellulosome to the cell surface. CipA binds to the anchor scaffoldin (OlpB,  
53 Orf2p or SdbA) via its type II dockerin. The anchor scaffoldins are attached to the cell by  
54 their SLH domains.

55  
56 Finally, CipA has one additional module, located between the 9<sup>th</sup> type I cohesin and the type II  
57 dockerin called the x-module. Its function in *C. thermocellum* remains unknown, although it has  
58 been shown to improve the solubility of recombinantly expressed type II dockerins and seems  
59 to enhance the affinity of the type II cohesin-dockerin interaction (7).

60 Electron microscopy has revealed hemispherical protuberances on the outside of *C.*  
61 *thermocellum* cells which are known as polycellulosomes (8). In their resting state they are  
62 about 200 nm in diameter, but form a protracted conformation in the presence of cellulose (9).  
63 Immunolabeling has identified the presence of CipA (10) and OlpB (6) in the polycellulosomes,  
64 though the protuberances may contain other cellulosomal components as well.

65 There have been two previous reports of mutants of *C. thermocellum* deficient in cellulase  
66 activity. Both were isolated by screening for cells unable to adhere to cellulose. *C.*  
67 *thermocellum* AD2 was isolated by mixing cells with cellulose and allowing the cellulose to  
68 settle. Adherent cells were pulled out of solution upon binding to cellulose, thus enriching the  
69 supernatant for non-adherent cells. After five rounds of this sedimentation enrichment, strain  
70 AD2 was isolated by single colony purification (11). The AD2 strain was analyzed by SDS-PAGE  
71 and found to be missing a band associated with CipA when grown on cellobiose, although the  
72 band reappeared when the strain was grown on cellulose (8). Further analysis of AD2 by  
73 scanning electron microscopy revealed the complete absence of polycellulosomes when grown  
74 on cellobiose (12).

75 Strains SM1, SM4, SM5 and SM6, also deficient in cellulase activity, were isolated using a  
76 procedure similar to that used for strain AD2, though augmented by an initial chemical  
77 mutagenesis step followed by a screen on cellobiose plates with an Avicel overlay (13). This  
78 final screen was designed to identify cells that were deficient in cellulose solubilization. These  
79 mutants were analyzed by SDS-PAGE and all were found to be missing a 210 kDa band  
80 associated with CipA. DNA sequence analysis revealed the presence of an IS1447 insertion

81 element disrupting the *cipA* coding sequence in each mutant. Strain SM1 had an insertion in  
82 the first type I cohesin and appeared to be completely lacking functional type I cohesins. This  
83 strain was unable to grow on MN300 cellulose and exhibited a 15-fold reduction in enzymatic  
84 activity compared to the wild type strain (13).

85 Previous work has shown that the ability to both bind and solubilize cellulose are linked (11,  
86 13). Thus, mutants deficient in cellulose-binding are also deficient in cellulose solubilization.  
87 The functional link between these abilities is consistent with our understanding of the  
88 component modules of CipA. In this study, we further evaluate the extent to which *cipA* is  
89 responsible for this dysfunctional phenotype and explore the cellulase activity of *C.*  
90 *thermocellum* in the absence of a complexed cellulase system.

## 91 **Materials and methods**

### 92 **Strains and media**

93 All *C. thermocellum* strains described here are derived from *C. thermocellum* strain DSM 1313  
94 and were grown in modified DSM 122 broth as described previously (14). Cellobiose or Avicel-  
95 PH105 microcrystalline cellulose (Sigma-Aldrich) was used as the primary carbon source at a  
96 concentration of either 5 or 10 g/l. Cells were grown at 55°C. Strain M1354 was a generous gift  
97 from the Mascoma Corporation (Lebanon, NH)(15). This strain is derived from *C. thermocellum*  
98 strain DSM 1313 and has a deletion of the *hpt* gene (Clo1313\_2927) to allow for use of the *hpt*  
99 gene as a counterselectable marker with the antimetabolite 8-azahypoxanthine.

## 100 **Molecular biological methods**

101 Plasmids were constructed using yeast mediated ligation (16), In-Fusion PCR cloning (Takara Bio  
102 Inc.), or standard cloning techniques(17). Plasmids were maintained in *E. coli* TOP10 cells  
103 (Invitrogen Corporation) and prepared using QIAGEN Plasmid Mini kit (QIAGEN Inc.). Sequences  
104 of chromosomal DNA were obtained by PCR using genomic DNA from *C. thermocellum* strain  
105 DSM 1313. Primers were designed using genome sequences provided by the Joint Genome  
106 Institute (<http://www.jgi.doe.gov/>). The *repB* and *cat* genes are derived from plasmid pMU102  
107 (18). The yeast origin of replication is derived from plasmid pMQ87 (16). The pMB1 *E. coli*  
108 origin of replication is derived from plasmid pUC19 (Invitrogen Corp.). The p15A *E. coli* origin of  
109 replication and arabinose-inducible promoter are derived from plasmid pBAD30 (19). The *hpt*  
110 and *tdk* genes (Tsac\_0936 and Tsac\_0324, respectively) are derived from  
111 *Thermoanaerobacterium saccharolyticum* JW/SL-YS485. The *gapDH<sub>p</sub>* promoter consists of the  
112 525 bp region upstream of the *C. thermocellum* glyceraldehyde 3-phosphate dehydrogenase  
113 gene (Clo1313\_2095). The *cbp<sub>p</sub>* promoter consists of the 621 bp region upstream of the  
114 cellobiose phosphorylase gene (Clo1313\_1954).

115 Plasmid pDGO-37 (GenBank accession number JX966413) was created by combining the p15A  
116 *E. coli* origin of replication and *Pbad* promoter with the thermophilic gram positive origin of  
117 replication from plasmid pMU102. Plasmid pDGO-40 (GenBank accession number JX966414)  
118 was created by inserting the *cipA* coding sequence, including 819 bp upstream of the start  
119 codon (putative promoter region) and 67 bp downstream of the stop codon (putative  
120 terminator region) into plasmid pDGO-37 (Fig. 1)(Table 1).

121 PCR was performed using either Taq or Phusion DNA polymerase (New England Biolabs Inc.)  
122 according to the directions provided by the manufacturer. When using whole cells as the PCR  
123 template, a 10-min heating step was included at the beginning of the thermocycling protocol to  
124 lyse the cells. When using Taq DNA polymerase, the lysing temperature was 95 °C. When using  
125 Phusion DNA polymerase, the lysing temperature was 98 °C. DNA sequencing was performed  
126 using standard techniques with an ABI Model 3100 genetic analyzer (Applied Biosystems).

### 127 **Strain construction**

128 Previously, two different deletions of *cipA* were made. In strain DS11, the *cipA* coding  
129 sequence was deleted from start to stop codon using plasmid pDGO-03 (GenBank accession  
130 number JX489218.1). In strain DS16, the *cipAp* promoter sequence was deleted in addition to  
131 the *cipA* coding region using plasmid pDGO-34 (Genbank accession number JX489219.1) (20).  
132 Plasmids were transformed into *C. thermocellum* using previously described techniques (21).  
133 To avoid the potential for homologous recombination between the plasmid and chromosomal  
134 copy of the *cipA* promoter region, plasmid pDGO-40 was only transformed into strain DS16.

### 135 **Fermentation conditions**

136 Strains were grown in modified DSM 122 broth (18) at 55°C with cellobiose or Avicel  
137 microcrystalline cellulose as the primary carbon source. When fermentations were performed  
138 in a 125 ml glass bottle sealed with a butyl rubber stopper (22), the fermentation volume was  
139 50 ml, 5 g/l substrate (Avicel or cellobiose) was used, the headspace was purged with nitrogen  
140 and the bottles were shaken at 200 rpm. When fermentations were performed in a computer-  
141 controlled fermenter (Sartorius GmbH), the fermentation volume was 2 L, 10 g/l substrate

142 (Avicel or cellobiose) was used, the headspace was purged with a mixture of 20% CO<sub>2</sub>, 80% N<sub>2</sub>,  
143 the vessel was stirred at 200 rpm and pH was controlled to 7.0 with 4N potassium hydroxide.  
144 For some fermentations, an automated sampling device was used to take 6 ml samples at  
145 regular intervals (23).

#### 146 **Analytical techniques**

147 Concentrations of cellobiose, glucose, lactate, acetate, ethanol and formate were measured by  
148 high performance liquid chromatography (HPLC) as previously described (24). Total carbon and  
149 total nitrogen concentrations were measured with a Shimadzu TOC-V CPH elemental analyzer  
150 with TNM-1 and ASI-V modules (Shimadzu Corp.) on 0.5-1.0 ml aliquots washed twice with  
151 water. Avicel concentration was determined from these measurements by assuming that  
152 Avicel contained no nitrogen and that cells contained carbon and nitrogen in a 4.67:1 molar  
153 ratio. A detailed description of the theory and calculations is being prepared for publication  
154 elsewhere (Holwerda and Lynd unpublished data).

155 Samples for protein identification were prepared as previously described (14). Briefly,  
156 cell pellets were separated from supernatant by centrifugation (2000 g) and washed twice with  
157 Tris-Buffered Saline (100 mM Tris HCl, 150 mM NaCl, pH 8.0) to remove residual supernatant  
158 proteins. Cells were lysed by the addition of SDS lysis buffer (SDS LB; 4% SDS [w/v] in 100 mM  
159 Tris HCl, pH 8.0), boiled (5 min), sonically disrupted (Branson), and boiled again. Supernatants  
160 were concentrated 50-fold (50 ml to 1 ml) via spin filtration using a 3 kDa MW cutoff  
161 membrane (Vivaspin 20, 3 kDa, PES [GE Healthcare]), adjusted to 2% SDS with 1 ml of SDS LB,  
162 and boiled (5 min). Both fractions, whole-cell (WC) and supernatant (SN), were precleared by



163 centrifugation (21000 g) and protein concentrations determined by BCA assay (Pierce). Sample  
164 fractions were then combined in a 2:1 WC to SN ratio (w/w), reduced with 25 mM dithiothreitol  
165 (DTT), and TCA precipitated (3 mg of combined crude lysate adjusted to 20% TCA on ice for 1  
166 hr). Precipitated proteins were then washed, resolubilized in denaturation buffer (8 M urea,  
167 100 mM Tris HCl, 5 mM DTT, pH 8.0), digested with trypsin and prepared for MudPIT LC-MS/MS  
168 as previously described (14). In total, 50 ug of peptides were analyzed per sample via a 24-hr  
169 MudPIT analysis using an LTQ XL mass spectrometer (Thermo Scientific). Resulting peptide  
170 fragmentation data was then searched with the MyriMatch database search algorithm (25)  
171 against the *C. thermocellum* DSM 1313 proteome (with decoy sequences) as previously  
172 described. Identified peptides were then score-filtered (FDR < 2% peptide spectrum match) and  
173 assembled into proteins identifications (minimum of 2 distinct peptides per protein call) by  
174 IDPicker 3 (26). Proteins were then spectrally balanced to deal with non-unique peptides,  
175 normalized by NSAF (normalized spectral abundance factors), and abundance values adjusted  
176 to nSpC (normalized spectral counts) as previously described (27). Protein-to-protein  
177 abundance was then assessed across all samples to identify those that were differentially  
178 expressed (Student's T test).

### 179 **Categorization of cellulase and cellulosomal proteins**

180 A list of all proteins that could participate in cellulose solubilization was generated, based on  
181 membership in the Carbohydrate Active Enzyme (CAZy) database (28) or presence of a cohesin  
182 or dockerin domain as determined by the Pfam database (29) (Supplemental dataset S1).  
183 Proteins with Pfam domain PF00963 were labeled as "cohesin-containing." Proteins with Pfam  
184 domain PF00404 (and no cohesin domain) were labeled as "dockerin-containing." Three

185 additional proteins, Clo1313\_1300, Clo1313\_2479 and Clo1313\_2861, were added to this list,  
 186 based on analysis done by Ed Bayer and colleagues (Ed Bayer, personal communication).  
 187 Proteins in the CAZy database that did not have a cohesin or dockerin domain were labeled as  
 188 “CAZy, no cohesin, no dockerin.”

### 189 **Mathematical analysis of fermentation data**

190 To determine the rate of substrate consumption, the substrate consumption data points were  
 191 fitted with the 5-parameter sigmoidal Richards equation(30) as described by Holwerda and  
 192 Lynd (unpublished data).

$$193 \quad s(t) = A_0 + \frac{A_t - A_0}{\left(1 + e^{\frac{t_0 - t}{slope}}\right)^{asymm}} \quad [1]$$

194 Where

195  $A_0$ = lower horizontal asymptote  
 196  $A_t$ = higher horizontal asymptote  
 197  $t$  = time  
 198  $x_0$ =inflection point  
 199 slope=slope at the inflection point  
 200 asymm= asymmetry parameter  
 201

202 The time ( $t$ ) when the slope of the fitted curve was greatest was determined by taking the 2<sup>nd</sup>  
 203 derivative with respect to time, setting it equal to zero and solving for  $t$ , which yielded the  
 204 following equation

$$205 \quad t_{\max slope} = x_0 + \ln(asymm) * slope \quad [2]$$

206 The first derivative of equation [1] with respect to time was then evaluated at the time  
 207 determined by equation [2] to determine the maximum rate of substrate consumption. To

208 allow ready comparison between Avicel and cellobiose, the substrate consumption rate was  
209 determined in mM glucose equivalent/hour.

## 210 **Results**

### 211 **Comparing growth rates of various mutants**

212 As expected, the wild type (WT) and *cipA* deletion strains (DS11 and DS16) have similar  
213 substrate consumption rates when grown on cellobiose (Fig. 2). The metabolic burdens of  
214 plasmid maintenance and thiamphenicol inactivation do not have an effect on Avicel  
215 consumption, as can be seen by comparing the wild type (strain WT) to the empty-vector  
216 control (strain DS19) (Fig. 2). The effect of *cipA* overexpression can be seen by comparing the  
217 empty-vector control (strain DS19) with the *cipA* overexpression strain (DS22). The rate of  
218 Avicel consumption was unchanged (Fig. 2). Deletion of *cipA* (strains DS11 and DS16) resulted  
219 in a 100-fold decrease in Avicel consumption rate when compared to the wild type strain (WT)  
220 (Fig. 2). Both *cipA* deletion strains were able to consume 80% of the Avicel initially present  
221 after ~2000 hours (Supplemental table S1 and supplemental figure S1). Fermentation products  
222 were similar to the parent strain (Supplemental table S2) and there was no significant  
223 accumulation of glucose or cellobiose. To see if the rate of Avicel consumption could be  
224 improved by adaptation, strain DS11 was subsequently passaged two additional times on  
225 Avicel, but no change in rate was detected.

226 Transforming the *cipA* deletion strain (DS16) with the *cipA* expression plasmid (pDGO-40,  
227 resulting in strain DS20) dramatically increased the rate of Avicel solubilization, although it was

228 still only 1/3 as fast as the empty vector control (DS19)(Fig. 2)(Supplemental table S1).  
229 Interestingly, there was a 100-hour lag phase before the start of rapid cellulose solubilization.  
230 The technique of measuring Avicel concentration by TOCN resulted in a larger degree of  
231 measurement variation during the early parts of fermentation. It is therefore difficult to  
232 determine whether slight negative trend observed in the first 100 hours with strain DS20  
233 represents a physical phenomenon or is simply an artifact of the measurement technique (Fig.  
234 3).

### 235 **Comparing protein abundance in various mutants**

236 Although the abundance was measured for all proteins (Supplemental dataset S1), only those  
237 proteins thought to be able to participate in cellulose solubilization (due to presence of a  
238 cohesin, dockerin or CAZy domain) were analyzed. The effect of the metabolic burdens of  
239 plasmid maintenance and antibiotic inactivation can be determined by comparing the empty  
240 vector control (strain DS19) to the wild type (WT) (Fig. 4, column 1). Among the cohesin-  
241 containing proteins, none are significantly differentially expressed. Among the dockerin-  
242 containing proteins, only Cel9F is significantly differentially expressed. Among the other CAZy  
243 proteins, only LicA is significantly differentially expressed.

244 The effect of *cipA* overexpression is demonstrated by comparing the empty vector control  
245 (strain DS19) with the *cipA* overexpression strain (strain DS22) (Fig. 4, column 2). Among the  
246 cohesin-containing proteins, none of them were significantly different at the 0.01 level.  
247 Although the increase in *cipA* expression was not significant at the 0.01 level ( $p=0.015$ ), when  
248 the values for the wild type (WT) are included as well, the significance increases to 0.0002,

249 suggesting that the effect would likely be confirmed if we were to perform more replicates.  
250 *CipA* expression increased by 3-fold in strain DS22, although this was not significantly different  
251 from the mean *cipA* expression in the empty-vector control (strain DS19) at the 0.01 level  
252 ( $p=0.015$ ). Among the dockerin-containing enzymes, none were significantly differently  
253 expressed at the 0.01 level. Among the other CAZy proteins, LicA and Clo1313\_0647 (CBM16-  
254 Domain of unknown function) were significantly lower in abundance.

255 The effect of *cipA* complementation can be determined by comparing the empty vector control  
256 (strain DS19) with the complemented *cipA* deletion strain (DS20) (Fig. 4, column 3). Among the  
257 cohesin-containing proteins, OlpB showed significantly reduced expression and was 11-fold less  
258 abundant in the complemented deletion strain. Among dockerin-containing proteins, Cel9P  
259 and Clo1313\_2861 (GH2-CBM6) showed increased expression. The significance of the  
260 Clo1313\_2861 result is difficult to interpret because of the low number of spectra identified for  
261 this protein ( $\leq 7$  for all samples). Among the other CAZy proteins, Clo1313\_2460 (GH15)  
262 showed significantly increased abundance.

263 Since OlpB contains 7 type II cohesins, a dramatic decrease in OlpB levels could result in a  
264 decrease in type II cohesin availability. Type II cohesin availability was calculated by multiplying  
265 the abundance of each anchor scaffoldin (SdbA, Orf2p and OlpB) by the number of type II  
266 cohesins it contains (Table 2).

267 **Discussion**

268 In agreement with Zverlov et al., we have shown that *cipA* is essential for rapid solubilization of  
269 crystalline cellulose(13). However, contrary to what was reported, we observed that *cipA*  
270 deletion strains are able to solubilize Avicel microcrystalline cellulose (which is similar to the  
271 MN300 microcrystalline cellulose used by Zverlov et al.). Furthermore, since the solubilization  
272 of Avicel resulted in the production of lactate, acetate and ethanol and this ability was  
273 maintained despite serial transfer, it appears that the strain was able to grow on Avicel. What  
274 is the explanation for residual ability of the *cipA* deletion strains (DS11 and DS16) to solubilize  
275 crystalline cellulose? One possibility is that components of the non-complexed cellulase system  
276 (i.e. Cell and CelY), which have been shown to synergistically solubilize crystalline cellulose (31),  
277 can compensate for the expected loss of activity. Since each enzyme has its own CBM, there is  
278 no need for CipA to mediate binding with the cellulosic substrate. These enzymes were found  
279 at very low levels in all strains (<0.01% of cell protein) as determined by nSpC values  
280 (Supplemental dataset S1), which reduces support for this explanation. Another possibility is  
281 that the cellulosomal components are bound directly to the cell surface via OlpA, which  
282 contains both a type I cohesin (for binding a cellulase enzyme containing a type I dockerin) and  
283 an s-layer homology (SLH) binding domain (for binding to the cell surface). Levels of OlpA were  
284 about 40% higher in the complemented *cipA* deletion strain (DS20) compared with the empty  
285 vector control (DS19), which supports this hypothesis.

286 Why does the *cipA* deletion and complementation strain (DS20) grow more slowly than the  
287 wild-type strain (WT) and have a longer lag phase? *CipA* expression doesn't seem to be a likely  
288 explanation, since minor variations in CipA abundance do not appear to be correlated with

289 growth rate (Fig. 5). On the other hand, OlpB levels were unexpectedly low in this strain.  
290 Compared to the empty-vector control strain (DS19), the *cipA* deletion and complementation  
291 strain (DS20) had 30% fewer type II cohesins, since it seems to have partly compensated for the  
292 reduction in *olpB* expression with higher levels of *sdbA* and *orf2p* expression. Furthermore, the  
293 wild type strain (WT) and the *cipA* overexpression strain (DS22) both had 15% fewer type II  
294 cohesins and this change in type II cohesin number did not have a substantial effect on  
295 fermentation performance, thus it seems unlikely that the change in type II cohesin number is  
296 the full explanation. Another possibility is that the anchor scaffoldins (OlpB, Orf2p and SdbA)  
297 are not, in fact, interchangeable. For example, if Orf2p and SdbA are primarily used during  
298 cellulosome assembly (as has been suggested for ORFXp in *Clostridium cellulolyticum* (32)) and  
299 OlpB is the final destination for the assembled cellulosome, then a change in the abundance of  
300 OlpB might have a greater impact on cellulosome function than would be indicated simply by  
301 the overall change in type II cohesin availability. Further investigations will be required to  
302 determine the exact molecular role of the various type II cohesin-containing proteins in  
303 cellulosome assembly.

304 Why is *olpB* expression changed in the *cipA* deletion strain? Although *cipA* and *olpB* have been  
305 reported to be transcribed independently (33), they may, in fact, be co-transcribed. Even if  
306 *cipA* and *olpB* are expressed from individual promoters, the 1 kb region upstream of *cipA* may  
307 contain other regulatory elements that affect *olpB* expression. Replacing the native *cipA*  
308 promoter on plasmid pDGO-40 with a different promoter would allow *cipA* to be expressed  
309 from a replicating plasmid in a *cipA* deletion strain where the native *cipA* promoter has been  
310 left on the chromosome (i.e. strain DS11).

311 The *cipA* deletion and complementation system described here will be useful for systematic  
312 understanding of the cellulolytic capabilities of *C. thermocellum*. The ability to express *cipA*  
313 from a replicating plasmid will enable the rapid exploration of the roles of its subcomponents  
314 including: elucidating the function of individual modules of *cipA*, exploration of alternative  
315 cellulosomal architectures and characterization of its non-complexed cellulase system.

316

### 317 **Acknowledgements**

318 We wish to thank Mr. Kyle Saltsman for his assistance with experimental work related to  
319 measuring growth rates.

320 The BioEnergy Science Center is a U.S. Department of Energy Bioenergy Research Center  
321 supported by the Office of Biological and Environmental Research, Genome Sciences Program  
322 in the DOE Office of Science.

### 323 **References**

324

- 325 1. **Demain AL, Newcomb M, and Wu JHD.** 2005. Cellulase, clostridia, and ethanol. *Microbiol. Mol.*  
326 *Biol. Rev.* **69**:124-154.
- 327 2. **Lamed R, Setter E, and Bayer EA.** 1983. Characterization of a cellulose-binding, cellulase-  
328 containing complex in *Clostridium thermocellum*. *J. Bacteriol.* **156**:828-836.
- 329 3. **Wu JHD, Orme-Johnson WH, and Demain AL.** 1988. Two components of an extracellular protein  
330 aggregate of *Clostridium thermocellum* together degrade crystalline cellulose. *Biochemistry*  
331 **27**:1703-1709.
- 332 4. **Gerngross UT, Romaniec MPM, Kobayashi T, Huskisson NS, and Demain AL.** 1993. Sequencing  
333 of a *Clostridium thermocellum* gene (*cipA*) encoding the cellulosomal S(L) protein reveals an  
334 unusual degree of internal homology. *Mol. Microbiol.* **8**:325-334.



- 335 5. **Tokatlidis K, Salamitou S, Beguin P, Dhurjati P, and Aubert JP.** 1991. Interaction of the  
336 duplicated segment carried by *Clostridium thermocellum* cellulases with cellulosome  
337 components. *FEBS Lett.* **291**:185-188.
- 338 6. **Lemaire M, Ohayon H, Gounon P, Fujino T, and Beguin P.** 1995. OlpB, a new outer layer protein  
339 of *Clostridium thermocellum*, and binding of Its S-layer-like domains to components of the cell-  
340 envelope. *J. Bacteriol.* **177**:2451-2459.
- 341 7. **Adams JJ, Pal G, Jia Z, and Smith SP.** 2006. Mechanism of bacterial cell-surface attachment  
342 revealed by the structure of cellulosomal type II cohesin-dockerin complex. *Proc. Natl. Acad. Sci.*  
343 *U. S. A.* **103**:305-310.
- 344 8. **Bayer EA, Setter E, and Lamed R.** 1985. Organization and distribution of the cellulosome in  
345 *Clostridium thermocellum*. *J. Bacteriol.* **163**:552-559.
- 346 9. **Bayer EA, Shimon LJW, Shoham Y, and Lamed R.** 1998. Cellulosomes--structure and  
347 ultrastructure. *J. Struct. Biol.* **124**:221-234.
- 348 10. **Bayer EA, and Lamed R.** 1986. Ultrastructure of the cell-surface cellulosome of *Clostridium*  
349 *thermocellum* and its interaction with cellulose. *J. Bacteriol.* **167**:828-836.
- 350 11. **Bayer EA, Kenig R, and Lamed R.** 1983. Adherence of *Clostridium thermocellum* to cellulose. *J.*  
351 *Bacteriol.* **156**:818-827.
- 352 12. **Lamed R, Naimark J, Morgenstern E, and Bayer EA.** 1987. Specialized cell-surface structures in  
353 cellulolytic bacteria. *J. Bacteriol.* **169**:3792-3800.
- 354 13. **Zverlov VV, Klupp M, Krauss J, and Schwarz WH.** 2008. Mutations in the scaffoldin gene, *cipA*,  
355 of *Clostridium thermocellum* with impaired cellulosome formation and cellulose hydrolysis:  
356 insertions of a new transposable element, IS1447, and implications for cellulase synergism on  
357 crystalline cellulose. *J. Bacteriol.* **190**:4321-4327.
- 358 14. **Olson DG, Tripathi SA, Giannone RJ, Lo J, Caiazza NC, Hogsett DA, Hettich RL, Guss AM,**  
359 **Dubrovsky G, and Lynd LR.** 2010. Deletion of the Cel48S cellulase from *Clostridium*  
360 *thermocellum*. *Proc. Natl. Acad. Sci. U. S. A.* **107**:17727-17732.
- 361 15. **Argyros DA, Tripathi SA, Barrett TF, Rogers SR, Feinberg LF, Olson DG, Foden JM, Miller BB,**  
362 **Lynd LR, Hogsett DA, and Caiazza NC.** 2011. High ethanol titers from cellulose by using  
363 metabolically engineered thermophilic, anaerobic microbes. *Appl. Environ. Microbiol.* **77**:8288-  
364 8294.
- 365 16. **Shanks RMQ, Caiazza NC, Hinsa SM, Toutain CM, and O'Toole GA.** 2006. *Saccharomyces*  
366 *cerevisiae*-based molecular tool kit for manipulation of genes from gram-negative bacteria. *Appl.*  
367 *Environ. Microbiol.* **72**:5027-5036.
- 368 17. **Maniatis T, Fritsch EF, and Sambrook J.** 1982. Molecular cloning: a laboratory manual. Cold  
369 Spring Harbor Laboratory, Cold Spring Harbor, NY.
- 370 18. **Tripathi SA, Olson DG, Argyros DA, Miller BB, Barrett TF, Murphy DM, McCool JD, Warner AK,**  
371 **Rajgarhia VB, Lynd LR, Hogsett DA, and Caiazza NC.** 2010. Development of *pyrF*-based genetic  
372 system for targeted gene deletion in *Clostridium thermocellum* and creation of a *pta* mutant.  
373 *Appl. Environ. Microbiol.* **76**:6591-6599.
- 374 19. **Guzman LM, Belin D, Carson MJ, and Beckwith J.** 1995. Tight regulation, modulation, and high-  
375 level expression by vectors containing the arabinose P<sub>BAD</sub> promoter. *J. Bacteriol.* **177**:4121-4130.
- 376 20. **Waller B, Olson DG, Currie DH, Guss A, and Lynd LR.** 2012. Exchange of type II dockerin-  
377 containing subunits of the *Clostridium thermocellum* cellulosome. *FEMS Microbiol. Lett.* **in**  
378 **press\***.
- 379 21. **Olson DG, and Lynd LR.** 2012. Chapter seventeen - transformation of *Clostridium thermocellum*  
380 by electroporation, p. 317-330. *In* H. J. Gilbert (ed.), *Methods Enzymol.*, vol. Volume 510.  
381 Academic Press.

- 382 22. **Hogsett DA.** 1995. Cellulose hydrolysis and fermentation by *Clostridium thermocellum* for the  
383 production of ethanol. Ph.D. thesis. Dartmouth College, Hanover, NH.
- 384 23. **Ellis LD.** 2011. Mass balances applied to cellulosic fermentations by *Clostridium thermocellum*  
385 (ATCC 27405) and the development of an automatic sampling system. M.S. thesis. Dartmouth  
386 College, Hanover.
- 387 24. **Zhang Y-HP, and Lynd LR.** 2005. Regulation of cellulase synthesis in batch and continuous  
388 cultures of *Clostridium thermocellum*. **187**:99-106.
- 389 25. **Tabb DL, Fernando CG, and Chambers MC.** 2007. MyriMatch: Highly accurate tandem mass  
390 spectral peptide identification by multivariate hypergeometric analysis. *J. Proteome Res.* **6**:654-  
391 661.
- 392 26. **Ma ZQ, Dasari S, Chambers MC, Litton MD, Sobel SM, Zimmerman LJ, Halvey PJ, Schilling B,**  
393 **Drake PM, Gibson BW, and Tabb DL.** 2009. IDPicker 2.0: improved protein assembly with high  
394 discrimination peptide identification filtering. *J. Proteome Res.* **8**:3872-3881.
- 395 27. **Lochner A, Giannone RJ, Keller M, Antranikian G, Graham DE, and Hettich RL.** 2011. Label-free  
396 quantitative proteomics for the extremely thermophilic bacterium *Caldicellulosiruptor*  
397 *obsidiansis* reveal distinct abundance patterns upon growth on cellobiose, crystalline cellulose,  
398 and switchgrass. *J. Proteome Res.* **10**:5302-5314.
- 399 28. **Cantarel BL, Coutinho PM, Rancurel C, Bernard T, Lombard V, and Henrissat B.** 2009. The  
400 Carbohydrate-Active EnZymes database (CAZy): an expert resource for glycogenomics. *Nucleic*  
401 *Acids Res.* **37**:233-238.
- 402 29. **Finn RD, Mistry J, Tate J, Coggill P, Heger A, Pollington JE, Gavin OL, Gunasekaran P, Ceric G,**  
403 **Forslund K, Holm L, Sonnhammer ELL, Eddy SR, and Bateman A.** 2010. The Pfam protein  
404 families database. *Nucleic Acids Res.* **38**:D211-D222.
- 405 30. **Richards FJ.** 1959. A flexible growth function for empirical use. *J. Exp. Bot.* **10**:290-301.
- 406 31. **Berger E, Zhang D, Zverlov VV, and Schwarz WH.** 2007. Two noncellulosomal cellulases of  
407 *Clostridium thermocellum*, Cel9I and Cel48Y, hydrolyse crystalline cellulose synergistically. *FEMS*  
408 *Microbiol. Lett.* **268**:194-201.
- 409 32. **Desvaux M.** 2005. The cellulosome of *Clostridium cellulolyticum*. *Enzyme. Microb. Technol.*  
410 **37**:373-385.
- 411 33. **Dror TW, Rolider A, Bayer EA, Lamed R, and Shoham Y.** 2003. Regulation of expression of  
412 scaffoldin-related genes in *Clostridium thermocellum*. *J. Bacteriol.* **185**:5109-5116.

413

414

415

## 416 **Figure legends**

417 **FIGURE 1** Diagram of genetic elements used in this work.

418 **FIGURE 2** Substrate consumption rate for strains of *C. thermocellum* grown on either cellobiose  
419 (cb) or Avicel (Av) at initial concentrations of 5 or 10 g/l. Antibiotic selection was used to  
420 maintain plasmid in plasmid-containing strains. The presence of the *cipA* coding sequence is  
421 indicated as either chromosomal (C), plasmid-based (P) or both. Error bars represent one  
422 standard deviation and were determined based on biological replicates, where  $n \geq 2$ .

423 \*Due to the difficulties of growing strains DS11 and DS16 on Avicel in fermenters, they were  
424 grown in sealed glass bottles instead.

425 **FIGURE 3** Avicel consumption of 4 strains of *C. thermocellum* growing on 10 g/l Avicel. In order  
426 to allow subsequent comparison with growth rates on cellobiose, the rate was reported in mM  
427 glucose equivalents per hour. Based on an assumed monomer mass of 162 g/mole and a 5%  
428 moisture content of Avicel, 58.6 mM glucose equivalents were present initially. Avicel  
429 consumption was measured by elemental analysis of the pellet fraction of fermentation broth  
430 corrected for cell carbon. Error bars represent one standard deviation,  $n=3$ , for Avicel  
431 measurement of a representative fermentation. Solid lines represent the best fit of a 5-  
432 parameter logistic equation. Equation parameters are given in Supplemental table S1.

433 **FIGURE 4** Comparison of protein abundance as determined by normalized spectral abundance  
434 factor (nSpC) from tandem mass spectrometry measurements of fermentation broth (combined  
435 cells and supernatant) at the end of Avicel fermentations. nSpC measurements were taken  
436 from biological duplicate experiments. Pairwise comparisons were made and proteins with  
437 significant changes ( $p < 0.01$ ) are indicated by filled symbols. Other proteins are indicated by

438 unfilled symbols. The presence of cohesins, dockerins and carbohydrate-binding modules  
 439 (CBMs) were determined by searching the Pfam database (29).

440 **FIGURE 5** Comparison of substrate consumption rate with the abundance of the CipA scaffoldin  
 441 protein for duplicate fermentations with strains DS1, DS19, DS20 and DS22 grown on 10 g/l  
 442 Avicel.

## 443 Tables

444 **TABLE 1** Description of strains

Strain	Chromosomal			Plasmid genetic		Genotype	Source
	genetic elements			elements			
	<i>cipAp</i>	<i>cipA</i>	<i>hpt</i>	<i>cat</i>	<i>cipAp-cipAt</i>		
WT	+	+	+			Wild type <i>C. thermocellum</i> DSM1313	DSMZ <sup>a</sup>
M1354	+	+				$\Delta hpt$	(15)
DS11	+					M1354 $\Delta cipA$	(20)
DS16						M1354 $\Delta(cipAp-cipA)$	(20)
DS18				+		DS16 /pDGO-37	This study
DS19	+	+		+		M1354/pDGO-37	This study
DS20				+	+	DS16/pDGO-40	This study
DS22	+	+		+	+	M1354 /pDGO-40	This study

445 <sup>a</sup>Deutsche Sammlung von Mikroorganismen und Zellkulturen GmbH, Germany.

446

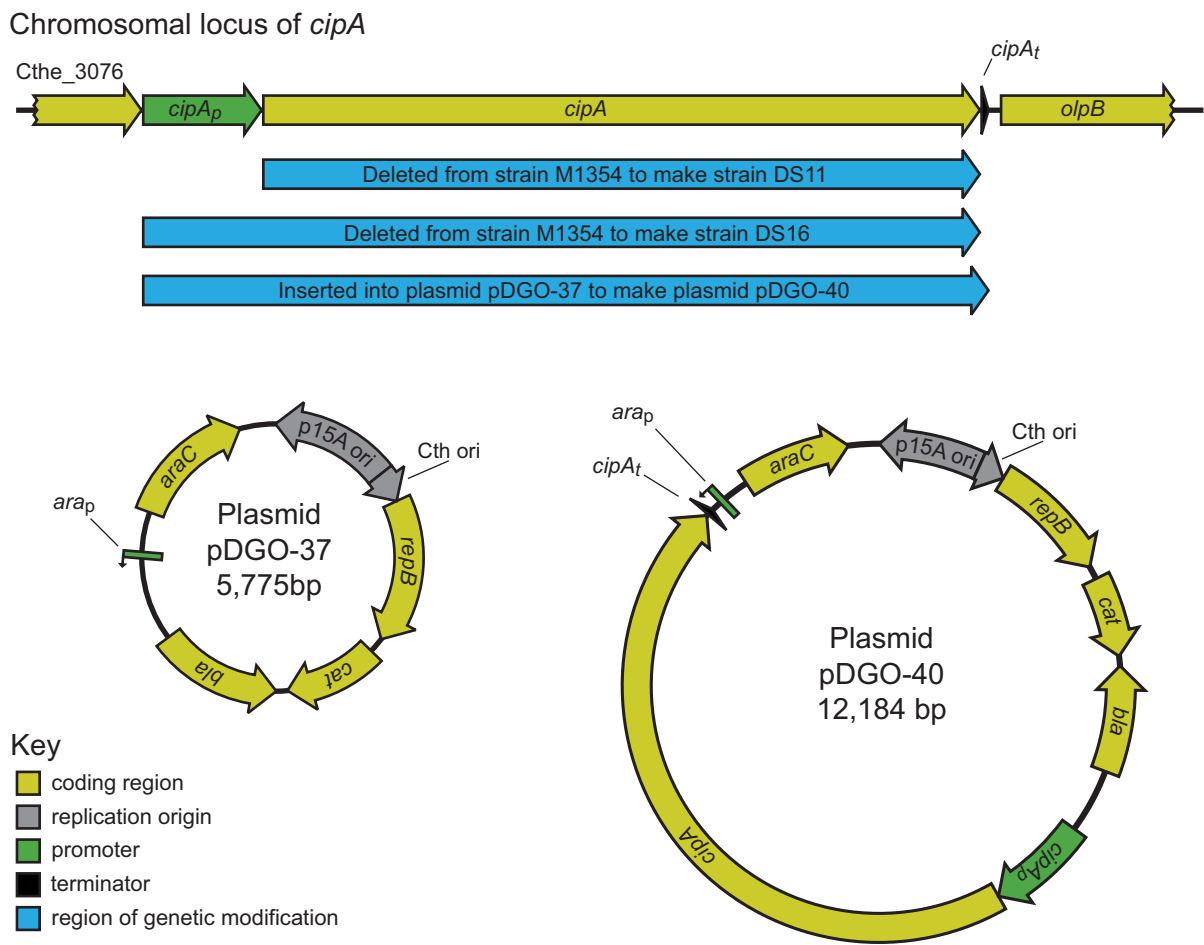
447 **TABLE 2** Abundance of type II cohesins

Name	Type II coh per molecule	Protein abundance (nSpC)			
		DS19	WT	DS20	DS22
SdbA	1	35.9	30.1	67.7	46.2
OlpB	7	44.1	42.0	3.8	38.7
Orf2p	2	106.3	70.8	148.1	77.9
<b>Total type II cohesins</b>		557.4	466.0	390.8	473.5

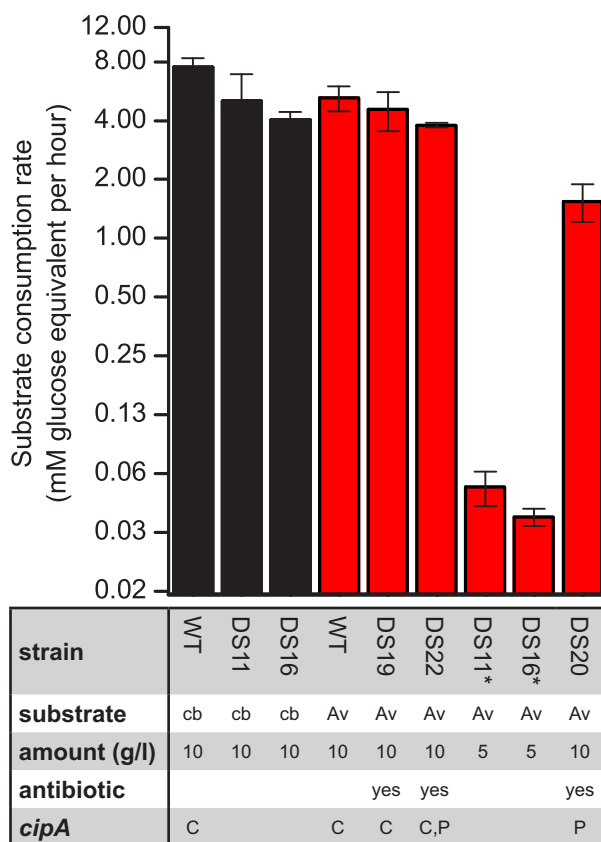
448

449

450

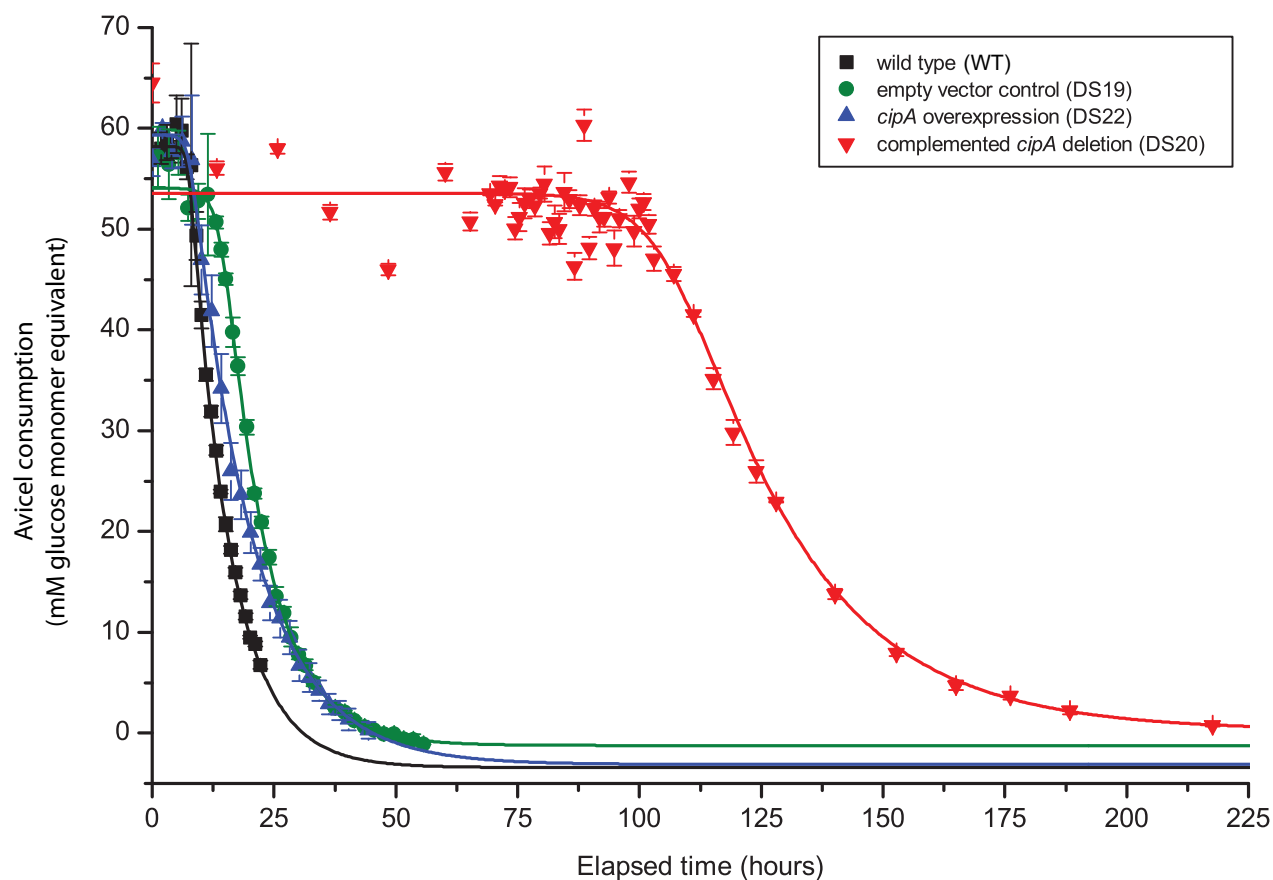


**FIGURE 1** Diagram of genetic elements used in this work



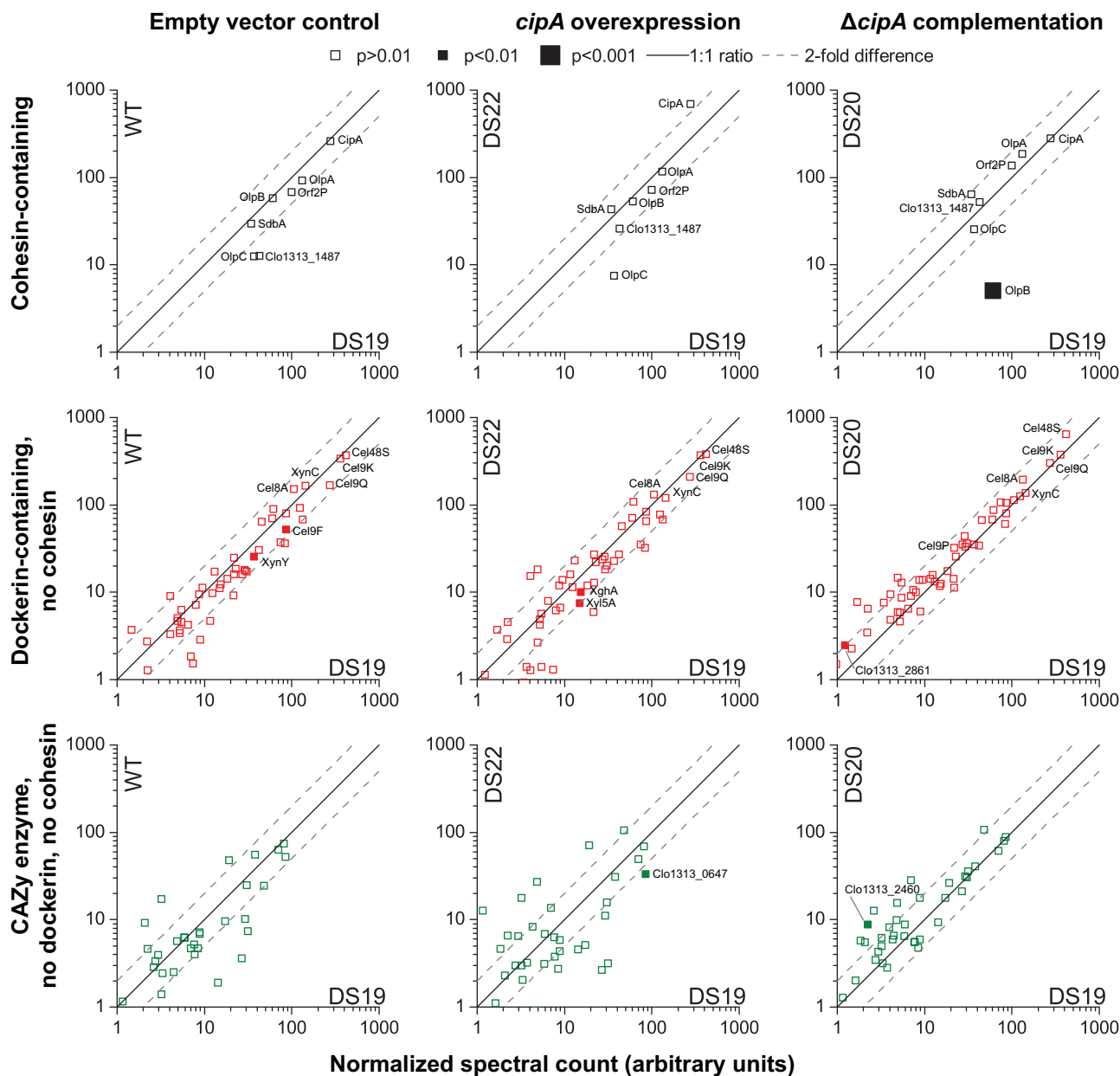
**FIGURE 2** Substrate consumption rate for strains of *C. thermocellum* grown on either cellobiose (cb, black bars) or Avicel (Av, red bars) at initial concentrations of 5 or 10 g/l. Antibiotic selection was used to maintain plasmid in plasmid-containing strains. The presence of the *cipA* coding sequence is indicated as either chromosomal (C), plasmid-based (P) or both. Error bars represent one standard deviation and were determined based on biological replicates, where  $n \geq 2$ .

\*Due to the difficulties of growing strains DS11 and DS16 on Avicel in fermenters, they were grown in sealed glass bottles instead.

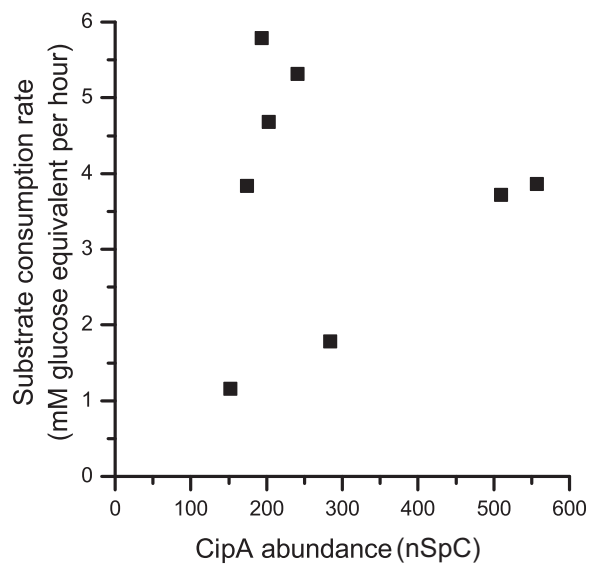


**FIGURE 3** Avicel consumption of 4 strains of *C. thermocellum* growing on 10 g/l Avicel. In order to allow subsequent comparison with growth rates on cellobiose, the rate was reported in mM glucose equivalents per hour. Based on an assumed monomer mass of 162 g/mole and a 5% moisture content of Avicel, 58.6 mM glucose equivalents were present initially. Avicel consumption was measured by elemental analysis of the pellet fraction of fermentation broth corrected for cell carbon. Error bars represent one standard deviation, n=3, for Avicel measurement of a representative fermentation. Solid lines represent the best fit of a 5-parameter logistic equation. Equation parameters are given in Supplementary material Table S1.





**FIGURE 4** Comparison of protein abundance as determined by normalized spectral abundance factor (nSpC) from tandem mass spectrometry measurements of fermentation broth (combined cells and supernatant) at the end of Avicel fermentations. nSpC measurements were taken from biological duplicate experiments. Pairwise comparisons were made and proteins with significant changes ( $p < 0.01$ ) are indicated by filled symbols. Other proteins are indicated by unfilled symbols. The presence of cohesins, dockerins and carbohydrate-binding modules (CBMs) were determined by searching the Pfam database.



Comparison of substrate consumption rate with the abundance of the CipA scaffoldin protein for duplicate fermentations with strains WT, DS19, DS20 and DS22 grown on 10 g/l Avicel.